Research Square

Preprints are preliminary reports that have not undergone peer review.
They should not be considered conclusive, used to inform clinical practice,
or referenced by the media as validated information.

Membranes or solution? Reassessing open-circuit voltage losses in a natural-water reverse electrodialysis pilot

Moulay Rachid Babaa

m.babaa@newuu.uz

New Uzbekistan University

Short Report

Keywords: Reverse electrodialysis, Open-circuit voltage, Membrane potential, Pitzer model, Electrolyte non-ideality, Natural waters

Posted Date: November 13th, 2026

DOI: https://doi.org/10.21203/rs.3.rs-11469384/v1

License: This work is licensed under a Creative Commons Attribution 4.0 International License.
Read Full License

Additional Declarations: Competing interest reported. Moulay Rachid Babaa is an inventor on Kazakhstan utility model patent No. 12564 (application No. 2026/0031.2, granted 10 July 2026), which relates to an Aral Sea brine management system based on reverse electrodialysis. This did not influence the study design, analysis or interpretation of the results. The author declares no other competing interests.

Membranes or solution? Reassessing open-circuit voltage losses in a natural-water reverse electrodialysis pilot

Moulay Rachid Babaa

Department of Chemical & Materials Engineering, New Uzbekistan University, Tashkent, Uzbekistan

Corresponding author: m.babaa@newuu.uz

Abstract

The open-circuit voltage (OCV) of a reverse electrodialysis (RED) stack reflects solution activities, membrane selectivity and the salinity gradients established during operation. The differences between measured and ideal OCV can arise from solution nonideality, imperfect membrane response and transport-induced changes in the local concentration gradients.. Published pilot data from Okinawa, with seawater or reverse-osmosis brine against river water, were reanalyzed with multicomponent Pitzer activities and independently measured membrane properties. Solution non-ideality and membrane response together account for only 19–33% of the deficit; the remaining 67–81% cannot be allocated with the available data. The split also depends on the ideal reference chosen for the river water, which is not NaCl-like. As a consequence, the OCV deficits obtained with natural waters should be reported together with their reference and interpreted only alongside independent membrane and stack measurements.

Keywords Reverse electrodialysis · Open-circuit voltage · Membrane potential · Pitzer model · Electrolyte non-ideality · Natural waters

Reverse electrodialysis (RED) converts the free energy of mixing of two salt solutions into electricity using alternating cation- and anion-exchange membranes (Weinstein and Leitz 1976; Post et al. 2008). The open-circuit voltage (OCV) is the simplest quantity measured on a stack and the one most often used for diagnosis. For a symmetric 1:1 electrolyte, each cation/anion-exchange membrane pair contributes two membrane potentials, and

$$E_{\mathrm{OCV}} = 2N\alpha_{\mathrm{eff}}\frac{RT}{F}\ln\left(\frac{a_{\pm,\mathrm{H}}}{a_{\pm,\mathrm{L}}}\right) + E_{\mathrm{el}} \quad (1)$$

where N is the number of cell pairs, α_{eff} an effective membrane-potential response factor, $a_{\pm,\mathrm{H}}$ and $a_{\pm,\mathrm{L}}$ the mean ionic activities of the concentrated and dilute feeds, E_{el} the electrode contribution (Veerman et al. 2010), R is the universal gas constant, T is the absolute temperature, and F is the Faraday constant. Here α_{eff} is a condition-specific factor for a stated concentration range, not an intrinsic permselectivity. With NaCl solutions, the measured OCV is routinely compared with Eq. (1) to benchmark membranes and stacks (Długołęcki et al. 2008; Veerman et al. 2009; Yip et al. 2014).

With natural waters the comparison is less simple. RED has now been operated at pilot scale with seawater, river water, desalination brine and saltworks brine (Tedesco et al. 2016, 2017; Kingsbury et al. 2017; Mehdizadeh et al. 2021). Multivalent ions alter membrane transport, can cause uphill transport and lower the voltage (Vermaas et al. 2014; Avci et al. 2016; Moreno et al. 2018), and at seawater and brine concentrations activities differ strongly from concentrations (Pitzer 1973; Pitzer and Mayorga 1973; Harvie et al. 1984). Hence, a low OCV can have several causes, yet the whole deficit is usually attributed either to solution non-ideality or to inferior membrane selectivity.

Distinguishing these contributions matters because solution non-ideality and membrane response have different implications for interpreting RED performance. It also affects comparisons between stacks operated with different natural waters, particularly when their ideal reference voltages are defined differently. The two lead to different research priorities and, for pilot plants, to different design choices. The attribution is also what is compared when stacks fed with different natural waters are ranked against each other, and such comparisons are only meaningful if the ideal voltage is defined in the same way. Published RED studies do not always use the same ideal-voltage reference, which can complicate comparisons of reported OCV deficits. The Okinawa pilot is one of the few published cases in which both the feed chemistry and the membrane pair were characterized independently,

which makes such a test possible. This work uses it to ask how much of a measured OCV deficit can actually be assigned to the solution and to the membranes, and how strongly the answer depends on the choice of ideal reference.

Activity coefficients were calculated with PHREEQC 3.8.6 and the pitzer.dat database (Harvie et al. 1984; Parkhurst and Appelo 2013) at 25 °C from the full reported compositions. For the NaCl component, $a_{\pm,\mathrm{NaCl}} = (a_{\mathrm{Na}}a_{\mathrm{Cl}})^{1/2}$ and $m_{\pm,\mathrm{NaCl}} = (m_{\mathrm{Na}}m_{\mathrm{Cl}})^{1/2}$, and the logarithmic driving force splits into an ideal and a non-ideal term:

$$\ln\left(\frac{a_{\pm,\mathrm{H}}}{a_{\pm,\mathrm{L}}}\right) = \ln\left(\frac{m_{\pm,\mathrm{H}}}{m_{\pm,\mathrm{L}}}\right) + \ln\left(\frac{\gamma_{\pm,\mathrm{H}}}{\gamma_{\pm,\mathrm{L}}}\right) \tag{2}$$

To compare the contributions on a common basis, three conditional allocation fractions are defined relative to the observed OCV deficit, $D = 1 - E_{\mathrm{meas}}/E_{\mathrm{ideal}}$. The activity correction is applied first: replacing the ideal driving force by the activity-based one removes the fraction $f_{\mathrm{act}} = -\ln(\gamma_{\pm,\mathrm{H}}/\gamma_{\pm,\mathrm{L}})/\ln(c_{\mathrm{H}}/c_{\mathrm{L}})$, where $c_{\mathrm{H}}/c_{\mathrm{L}}$ is the ideal concentration ratio of the chosen reference. The activity-corrected voltage is then multiplied by the assumed membrane-response factor α_{eff}, and the remaining difference is designated as the unallocated residual:

$$S_{\mathrm{act}} = \frac{f_{\mathrm{act}}}{D}, \quad S_{\mathrm{mem}} = \frac{(1-\alpha_{\mathrm{eff}})(1-f_{\mathrm{act}})}{D}, \quad S_{\mathrm{res}} = 1 - S_{\mathrm{act}} - S_{\mathrm{mem}} \tag{3}$$

These fractions are an accounting convention not a unique physical decomposition of the measured voltage deficit. Their values depend on the chosen ideal-voltage reference and on the assumed membrane-response factor, and the residual includes effects that cannot be separated with the available measurements. The source data, the calculation sequence and the sensitivity cases are given in the Supplementary Information.

Mehdizadeh et al. (2021) fed a 299-cell-pair pilot stack in Okinawa with river water (RW), seawater (SW) and reverse-osmosis (RO) brine. At the highest flow rate the measured OCV was about 65% of the theoretical inlet value for SW/RW and 60% for RO-brine/RW, and the authors noted that it approached the theoretical outlet OCV. Sugimoto et al. (2022) later characterized the same CIMS/ACS-8T membrane pair, allowing a conditional partition of the OCV deficit using independently reported membrane measurements instead of parameters fitted to the pilot data. The partition however depends on transferring the membrane-response factors from laboratory NaCl solutions to the natural pilot feeds. The stack equation printed by Mehdizadeh et al. (2021) lacks the factor of two in Eq. (1), although N is defined there as the number of cell pairs; per-pair voltages reported for the same membrane pair favor the full-pair interpretation, which was adopted (Section S3). The seawater K^+ concentration was kept at the reported 33 mmol L^{-1}; an independent analysis of Chatan seawater gave a comparably elevated 29 mmol L^{-1} (Sugimoto et al. 2022). The analyses have charge-balance errors of 40.8%, 9.18% and −3.55% for RW, SW and RO brine. Assigning the RW anion deficit to HCO_3^- changes the mean NaCl activity coefficient of RW only from 0.935 to 0.934, and the activity shares by at most 0.1 percentage points, so the reported compositions were used as published (Section S4).

The Pitzer calculation gives $\ln(\gamma_{\pm,H}/\gamma_{\pm,L}) \approx -0.34$ for SW/RW and −0.36 for RO-brine/RW, and Using molal instead of molar concentrations changes the ideal driving force by less than 0.4%. The more important difference comes from how the ideal voltage is defined.

We considered two references. The first follows the original pilot study and represents each water sample by a NaCl solution with the same conductivity. With this reference, the measured OCV is 62.5% of the ideal value for SW/RW and 57.9% for RO-brine/RW. The

second reference uses the measured Na^+ and Cl^- concentrations to calculate the ideal voltage. It gives lower ratios of 52.5% and 48.8%, respectively.

The difference comes mainly from the river water. Its conductivity corresponds to approximately 2.9 mmol L^{-1} NaCl, whereas its Na–Cl mean concentration is only about 0.94 mmol L^{-1}. This difference changes the ideal logarithmic driving force by roughly one unit, which is larger than the Pitzer activity correction itself.

As a result, changing from the conductivity-based to the composition-based reference increases the calculated OCV deficit from 37.5% to 47.5% for SW/RW and from 42.1% to 51.2% for RO-brine/RW. At the same time, the share attributed to solution nonideality decreases from 17.2% to 11.4% and from 14.9% to 10.3%, respectively (Table 1). The two references do not have the same thermodynamic meaning. The composition-based reference gives an exact decomposition of the modeled Na–Cl mean activity contrast, because the concentration and activity terms are defined consistently. The conductivity-based reference is useful for comparison with the original pilot study, but its allocation of the deficit is diagnostic rather than an exact thermodynamic decomposition (Table S4).

Table 1 Partition of the Okinawa ideal-to-measured OCV deficit for two ideal references

				Share of deficit (%)[a]		
Gradient	Ideal reference	E_{meas}/E_{ideal}	Deficit (%)	Activity	Membrane	Unallocated residual[b]
SW/RW	Conductivity-equivalent	0.625	37.5	17.2	10.0	72.8
	Composition ($m_{\pm,NaCl}$)	0.525	47.5	11.4	8.0	80.6
RO-brine/RW	Conductivity-equivalent	0.579	42.1	14.9	17.8	67.3
	Composition ($m_{\pm,NaCl}$)	0.488	51.2	10.3	14.8	74.9

[a] Conditional allocations from Eq. (3), activity correction first. Only the composition rows decompose Eq. (2) exactly; the conductivity-equivalent rows are reference-dependent diagnostic allocations (calculation sequence in Table S4); reversing the order shifts at most 1.2 percentage points between the activity and membrane shares and leaves the residual unchanged. [b] Not measured independently.

Sugimoto et al. (2022) report ion transport numbers of 0.98 for both CIMS and ACS-8T, which in the binary monovalent approximation corresponds to $2t - 1 \approx 0.96$. They also

measured single-membrane potentials between NaCl solutions of 90 and 1.50 mS cm^{-1}, about 102 mV for the cation-exchange and 91 mV for the anion-exchange membranes, or about 7.7 V for 40 pairs against an ideal 8.4 V. These results are represented by approximate response factors, $\alpha_{eff} \approx 0.96$ for SW/RW and 0.92 for RO-brine/RW. Membrane response then accounts for 10.0% and 17.8% of the deficit with the conductivity-equivalent reference, and for 8.0% and 14.8% with the composition reference (Table 1, Fig. 1). The factors come from model NaCl solutions, and multivalent ions could lower the response in the natural feeds (Vermaas et al. 2014; Avci et al. 2016), but this has not been measured. Each 0.01 decrease in α_{eff} moves about 2 percentage points from the residual to the membrane share, and the residual stays above half of the deficit unless α_{eff} falls below 0.79–0.87 (Section S4). Under the assumed ±0.01 perturbation of the measured-to-ideal voltage ratio, the resulting change in the residual allocation is smaller than the changes associated with the choice of reference and membrane-response assumptions.

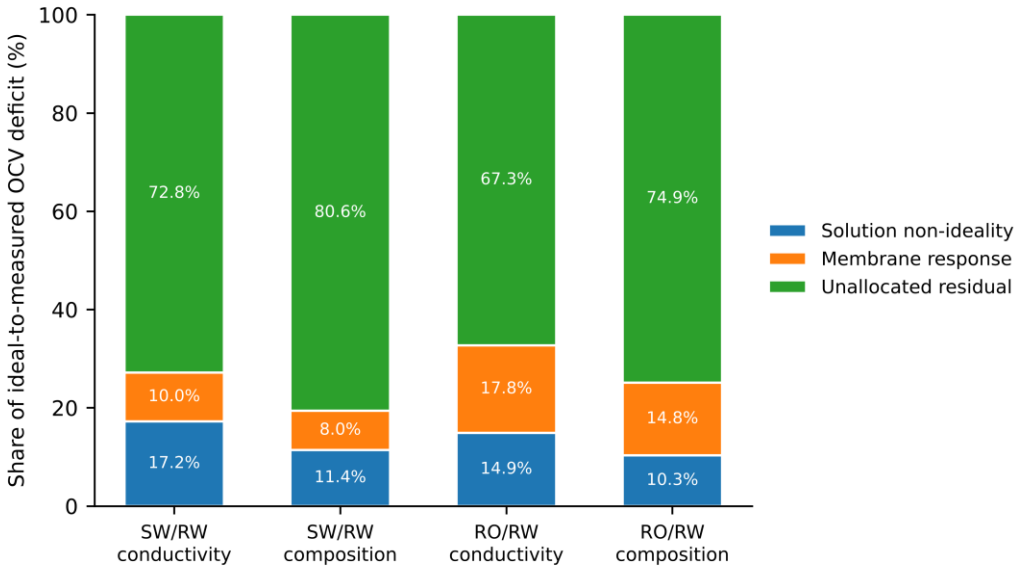


Fig. 1 Partition of the Okinawa ideal-to-measured OCV deficit for two ideal references. Percentages are expressed relative to the total deficit, ($D = 1 - E_{meas}/E_{ideal}$), rather than the absolute stack voltage. The Pitzer activity correction is applied first and the membrane-response factor ($\alpha_{eff} \approx 0.96$ and 0.92) second. Composition bars decompose Eq. (2) exactly; conductivity-equivalent bars are diagnostic allocations. The unallocated residual was not measured independently

The remaining 67.3–80.6% is an unallocated difference between model and measurement, not a quantified loss. It may include axial relaxation of the salinity gradient, polarization, water and salt transport not captured by α_{eff} and electrode effects, and it also absorbs any error in the ideal reference and in transferring laboratory membrane data to the pilot. Its size is consistent with the observation that the measured OCV approached the theoretical outlet OCV (Mehdizadeh et al. 2021) and with the known dependence of stack voltage on flow rate and residence time (Veerman et al. 2009; Vermaas et al. 2013). The highest flow rate reported for the Okinawa pilot does not establish that the inlet thermodynamic voltage was approached. Although increasing flow can reduce axial concentration changes, the available measurements do not determine how much of the remaining deficit would persist at still higher flow rates. A single fitted membrane parameter cannot separate these terms: an ideal Donnan model fitted to the SW/RW stack ratio needs an effective fixed-charge density an order of magnitude below the value implied by the measured membrane response suggesting that the fitted parameter compensates for effects not represented in the simplified Donnan model (Section S5).

These results bear directly on how RED data from natural waters are reported and compared. Feed analyses should include alkalinity, state whether concentrations are molar or molal, and give the charge-balance error. When the dilute feed is not NaCl-like, the ideal OCV should be reported for at least two references, with the way it was calculated. Static membrane potentials measured with the actual membrane pair in the actual feeds give α_{eff} independently, and OCVs at several flow rates, together with inlet and outlet theoretical OCVs, bound the axial relaxation of the gradient. For hypersaline brines, reducing a multicomponent composition to a single NaCl equivalent adds a further ambiguity that is outside the scope of this study.

In conclusion, the Okinawa pilot data leave between two thirds and four fifths of the OCV deficit unexplained by solution non-ideality or membrane response, and the split between the explained parts moves with the choice of ideal reference. The OCV of a well-characterized stack could serve as an in situ check on activity models for natural waters, but only once the membrane response and the salinity profile along the stack have been measured separately. Without such measurements, assigning the deficit to non-ideality or to the membrane remains an assumption, and deficits reported without their reference cannot be compared between studies.

Supporting information The Supplementary Information contains the source compositions and charge-balance sensitivity, the cell-pair convention, the deficit partition with its calculation sequence and sensitivities, and the Donnan check.

Funding No funds, grants, or other support was received.

Declarations

Conflict of interest Moulay Rachid Babaa is an inventor on Kazakhstan utility model patent No. 12564 (application No. 2026/0031.2, granted 10 July 2026), which relates to an Aral Sea brine management system based on reverse electrodialysis. This did not influence the study design, analysis or interpretation of the results. The author declares no other competing interests.

Author contributions Moulay Rachid Babaa: conceptualization, methodology, formal analysis, visualization, writing – original draft, writing – review and editing.

Data availability The input data, calculation scripts, numerical results, figures and reproducibility instructions supporting this study are provided in the accompanying Supplementary Materials. The computational package includes the files required to reproduce the reported calculations and figures.

Ethics approval Not applicable. This study reanalyzes previously published data and did not involve human participants or animals.

Use of AI tools During the preparation of this manuscript, the author used Grammarly to improve language and readability. The author reviewed and edited the text and takes full responsibility for the content of the publication.

References

Avci AH, Sarkar P, Tufa RA, Messana D, Argurio P, Fontananova E, Di Profio G, Curcio E (2016) Effect of Mg^{2+} ions on energy generation by reverse electrodialysis. J Membr Sci 520:499–506. https://doi.org/10.1016/j.memsci.2016.08.007

Długołęcki P, Nymeijer K, Metz S, Wessling M (2008) Current status of ion exchange membranes for power generation from salinity gradients. J Membr Sci 319:214–222. https://doi.org/10.1016/j.memsci.2008.03.037

Harvie CE, Møller N, Weare JH (1984) The prediction of mineral solubilities in natural waters: the Na–K–Mg–Ca–H–Cl–SO_4–OH–HCO_3–CO_3–CO_2–H_2O system to high ionic strengths at 25 °C. Geochim Cosmochim Acta 48:723–751. https://doi.org/10.1016/0016-7037(84)90098-X

Kingsbury RS, Liu F, Zhu S, Boggs C, Armstrong MD, Call DF, Coronell O (2017) Impact of natural organic matter and inorganic solutes on energy recovery from five real salinity gradients using reverse electrodialysis. J Membr Sci 541:621–632. https://doi.org/10.1016/j.memsci.2017.07.038

Mehdizadeh S, Kakihana Y, Abo T, Yuan Q, Higa M (2021) Power generation performance of a pilot-scale reverse electrodialysis using monovalent selective ion-exchange membranes. Membranes 11:27. https://doi.org/10.3390/membranes11010027

206 Moreno J, Díez V, Saakes M, Nijmeijer K (2018) Mitigation of the effects of multivalent ion
207 transport in reverse electrodialysis. J Membr Sci 550:155–162.
208 https://doi.org/10.1016/j.memsci.2017.12.069
209 Parkhurst DL, Appelo CAJ (2013) Description of input and examples for PHREEQC version
210 3. U.S. Geological Survey Techniques and Methods, book 6, chap. A43.
211 https://doi.org/10.3133/tm6A43
212 Pitzer KS (1973) Thermodynamics of electrolytes. I. Theoretical basis and general equations.
213 J Phys Chem 77:268–277. https://doi.org/10.1021/j100621a026
214 Pitzer KS, Mayorga G (1973) Thermodynamics of electrolytes. II. Activity and osmotic
215 coefficients for strong electrolytes with one or both ions univalent. J Phys Chem
216 77:2300–2308. https://doi.org/10.1021/j100638a009
217 Post JW, Hamelers HVM, Buisman CJN (2008) Energy recovery from controlled mixing salt
218 and fresh water with a reverse electrodialysis system. Environ Sci Technol 42:5785–
219 5790. https://doi.org/10.1021/es8004317
220 Sugimoto Y, Ujike R, Higa M, Kakihana Y, Higa M (2022) Power generation performance of
221 reverse electrodialysis (RED) using various ion exchange membranes and power output
222 prediction for a large RED stack. Membranes 12:1141.
223 https://doi.org/10.3390/membranes12111141
224 Tedesco M, Scalici C, Vaccari D, Cipollina A, Tamburini A, Micale G (2016) Performance of
225 the first reverse electrodialysis pilot plant for power production from saline waters and
226 concentrated brines. J Membr Sci 500:33–45.
227 https://doi.org/10.1016/j.memsci.2015.10.057
228 Tedesco M, Cipollina A, Tamburini A, Micale G (2017) Towards 1 kW power production in a
229 reverse electrodialysis pilot plant with saline waters and concentrated brines. J Membr
230 Sci 522:226–236. https://doi.org/10.1016/j.memsci.2016.09.015

231 Veerman J, Saakes M, Metz SJ, Harmsen GJ (2009) Reverse electrodialysis: performance of a
232 stack with 50 cells on the mixing of sea and river water. J Membr Sci 327:136–144.
233 https://doi.org/10.1016/j.memsci.2008.11.015
234 Veerman J, Saakes M, Metz SJ, Harmsen GJ (2010) Reverse electrodialysis: evaluation of
235 suitable electrode systems. J Appl Electrochem 40:1461–1474.
236 https://doi.org/10.1007/s10800-010-0124-8
237 Vermaas DA, Veerman J, Saakes M, Nijmeijer K (2014) Influence of multivalent ions on
238 renewable energy generation in reverse electrodialysis. Energy Environ Sci 7:1434–
239 1445. https://doi.org/10.1039/C3EE43501F
240 Vermaas DA, Veerman J, Yip NY, Elimelech M, Saakes M, Nijmeijer K (2013) High
241 efficiency in energy generation from salinity gradients with reverse electrodialysis. ACS
242 Sustain Chem Eng 1:1295–1302. https://doi.org/10.1021/sc400150w
243 Weinstein JN, Leitz FB (1976) Electric power from differences in salinity: the dialytic
244 battery. Science 191:557–559. https://doi.org/10.1126/science.191.4227.557
245 Yip NY, Vermaas DA, Nijmeijer K, Elimelech M (2014) Thermodynamic, energy efficiency,
246 and power density analysis of reverse electrodialysis power generation with natural
247 salinity gradients. Environ Sci Technol 48:4925–4936.
248 https://doi.org/10.1021/es5005413

Supplementary Files

This is a list of supplementary files associated with this preprint. Click to download.

- REDOCVChemPapsubmissionpackage1.zip
- SupplementaryInformationBabaaChemPap3.docx